Article
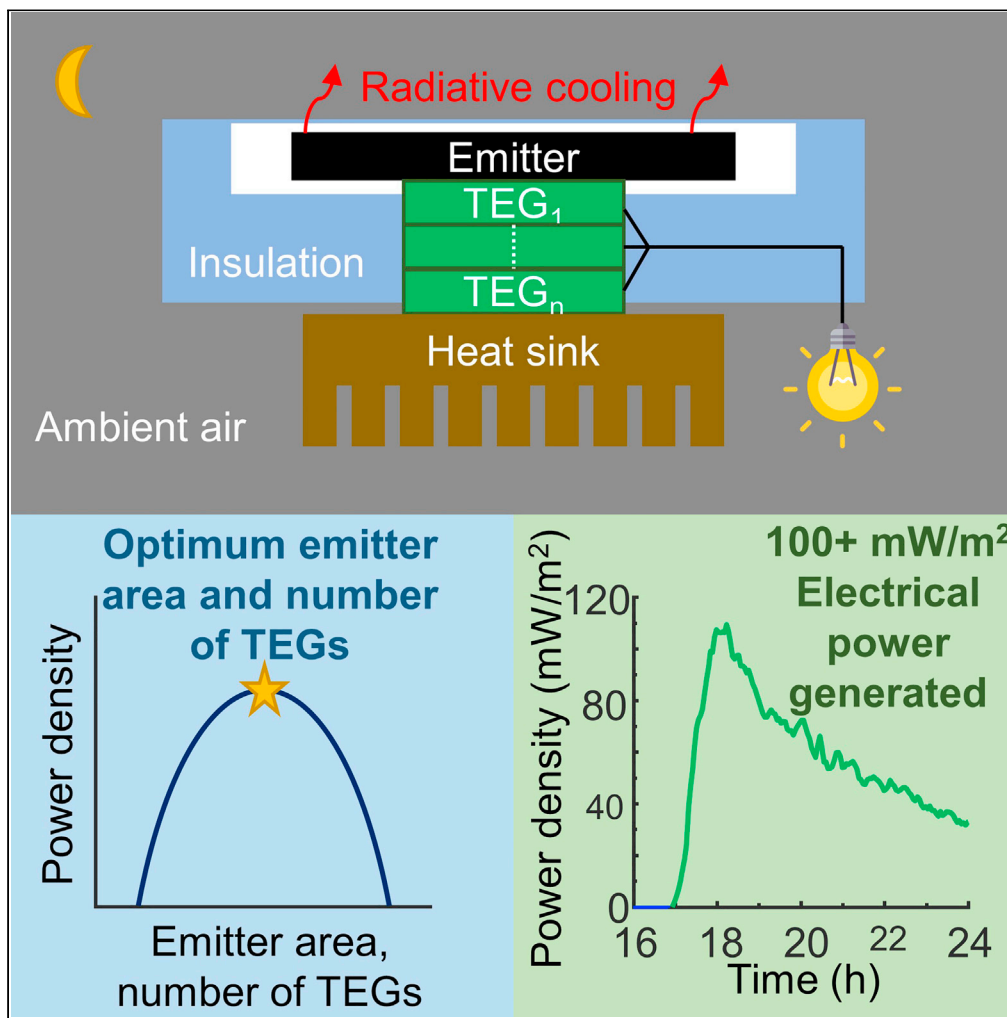
Radiative-cooling-based nighttime electricity generation with power density exceeding 100 mW/m^2

Zunaid Omair, Sid Assawaworrarit, Lingling Fan, Weiliang Jin, Shanhui Fan

shanhui@stanford.edu

Highlights

We demonstrate >100 mW/m^2 power generation at nighttime from radiative cooling

This power density is four times over the previous record

Key is to optimize outgoing thermal radiation over parasitic heat transfer channels

Proposed model allows system design with maximal power generation at nighttime

Article

Radiative-cooling-based nighttime electricity generation with power density exceeding 100 mW/m²

Zunaid Omair,[1] Sid Assawaworrarit,[1] Lingling Fan,[1] Weiliang Jin,[1] and Shanhui Fan[1,2,*]

SUMMARY

The outer space (3 K) represents an important thermodynamic resource. It has been known for decades that at nighttime, a sky-facing thermal emitter radiating strongly within the atmospheric transparency window (8–13 μm), can reach below the ambient temperature. In recent studies, thermoelectric generators were used to harness this temperature difference between the emitter and ambient to generate electricity. However, the demonstrated power density has been limited by parasitic thermal losses. Here we show that these parasitic losses can be reduced through thermal engineering. We present a simple model showing the optimum power density can be approached by controlling the relation between the emitter area and the thermal resistance of the thermoelectric generator. We show that the stacking of multiple thermoelectric generators is an effective way to approach this optimum. We experimentally demonstrate a generated electric power density >100 mW/m², representing > 2-fold improvement over the previous results for nighttime radiative cooling.

INTRODUCTION

Nighttime renewable energy harvesting represents a significant engineering challenge. Daytime energy generation, by harvesting sunlight, has made tremendous progress over the last two decades (Green et al., 2022). Meanwhile, the standard way to provide renewable energy at night is through energy storage (Bowen et al., 2021). However, in many applications, the possibilities for renewable energy generation without the need for storage are attractive in terms of reducing system complexity or cost.

At night, as the sunlight is absent, to provide power, one needs another source of energy from the ambient environment. Technologies such as wind (Holmes et al., 2004) and radio-frequency harvesting (Yeatman, 2004; Ajmal et al., 2014) have been proposed and tested. But the achieved power density (power generated/area), which represents a critical figure-of-merit of ambient energy harvesting, remains low. The maximum power density demonstrated for wind is 177 μW/m² (Holmes et al., 2004), and for radio-frequency harvesting, it is 2 mW/m² (Ajmal et al., 2014). Further increasing the power density is important for applications such as night-time lighting or providing power to off-grid sensors.

In recent years there have been emerging interests in harvesting the coldness of the universe as a thermodynamic resource (Rephaeli et al., 2013; Zhu et al., 2013, 2014, 2015; Byrnes et al., 2014; Raman et al., 2014, 2019; Shi et al., 2015; Hossain and Gu, 2016; Li et al., 2017, 2018a, 2018b, 2019, 2020a, 2020b, 2020c, 2021; Zhai et al., 2017; Buddhiraju et al., 2018; Hu et al., 2018; Mandal et al., 2018, 2020; Tsoy et al., 2018; Zhao et al., 2018, 2019; Li and Fan, 2019; Ono et al., 2019; Dong et al., 2019; Zhou et al., 2019; Fan et al., 2020; Yin et al., 2020; Ishii et al., 2020; Fan and Li, 2022; Assawaworrarit et al., 2022). The outer space, at a temperature of 3 K, represents an important thermodynamic resource. Moreover, with a clear sky, outgoing thermal radiation can efficiently transfer heat from the Earth's surface to the cold sink of outer space. Thus, an object located on the Earth's surface does have radiative access to the outer space. Such outgoing thermal radiation can be harvested to generate work using a heat engine located at the Earth's surface. Theoretically, it was noted that a thermal engine, in thermal contact with a heat source at a temperature of 300 K (approximating that of the Earth's surface), radiating to a heat sink of 3 K (approximating that of the outer space), can generate work with power density ranging from 48.4

[1]Edward L. Ginzton Laboratory, Stanford University, Stanford, CA 94305, USA

[2]Lead contact

*Correspondence: shanhui@stanford.edu

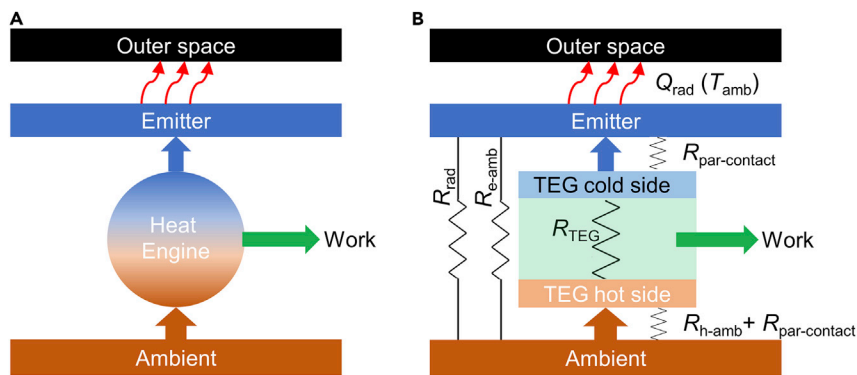https://doi.org/10.1016/j.isci.2022.104858

Figure 1. Nighttime energy harvesting using radiative cooling

(A) Schematic of the harvesting process with a heat engine that generates work using the temperature difference between the ambient and the emitter.

(B) A thermal model showing various thermal exchange pathways and the corresponding thermal resistances, when a thermoelectric generator (TEG) is used as a heat engine.

W/m^2 to 153.1 W/m^2, at various thermodynamic limits (Byrnes et al., 2014; Buddhiraju et al., 2018). As radiative access to the outer space is present both day and night, it is interesting to exploit the outer space for nighttime power generation.

Experimentally, it has been known for many decades that a black thermal emitter facing the sky can reach a temperature that is 10-15°C below the ambient air temperature (Granqvist and Hjortsberg, 1981; Eriksson and Granqvist, 1982; Eriksson et al., 1984). More recently, Chen et al. (2016) have demonstrated a temperature reduction of 40°C below the ambient air temperature, using a selective emitter enclosed by a vacuum chamber. Based on these nighttime radiative cooling effects, Raman et al. (2019) generated electricity from the temperature difference between the ambient with a thermoelectric generator and achieved a power density of 25 mW/m^2. Improving upon the setup design, Assawaworrarit et al. (2022) demonstrated a power density of 50 mW/m^2, using a solar cell as the radiative emitter. Radiative-cooling-based nighttime power generation has also been explored by a number of other experiments (Ono et al., 2019; Zhao et al., 2020; Zhao et al., 2021; Yu et al., 2022; Ishii et al., 2020; Deppe and Munday, 2020; Khan et al., 2021; Liao et al., 2022).

In this article, we show in detail the thermal considerations necessary for a system generating electricity at night using radiative cooling. We provide an optimization model for maximum power density harvesting and propose methods to reduce parasitic heat transfers. We demonstrate >100 mW/m^2 power generation at nighttime, which represents a significant advancement in the quest of using radiative cooling to generate electricity.

Theoretical analysis

Radiative-cooling-based nighttime power generation has been analyzed in Raman et al., 2019; Assawaworrarit et al., 2022; Chen et al., 2016. In this work, we provide a simplified model that highlights the considerations in thermal engineering of the energy harvesting system.

A conceptual description of the nighttime energy harvesting process is shown in Figure 1A. Here, an emitter facing the night sky reaches a temperature below the ambient. And a heat engine is then used to extract work from the temperature difference between the ambient and the emitter.

In this work, we use a thermoelectric generator (TEG) (Disalvo, 1999) as the heat engine (Figure 1B). To extract heat efficiently from the Earth, the hot side of the TEG should be in good thermal contact with the Earth, i.e., the ambient air. We denote the thermal resistance of this heat transfer process as R_h. The cold side of the TEG is in contact with an emitter performing radiative cooling. We denote the thermal resistance of this heat transfer process as R_c. Both R_h and R_c can include contact thermal resistance at the respective interfaces. These contact thermal resistances can cause temperature drops at the interfaces, thereby losing useful energy.

The radiative cooling power density of the emitter is the balance between the outgoing radiation power density of the emitter (at temperature T_{emit}), $q_{emit}(T_{emit})$, and the incoming radiation power density from the Earth's atmosphere (at temperature T_{amb}) absorbed by the emitter, $q_{atm}(T_{amb})$, resulting in net radiative cooling power density $q_{rad}(T_{emit}) = q_{emit}(T_{emit}) - q_{atm}(T_{amb})$. In the full model (Raman et al., 2019; Assawaworrarit et al., 2022; Chen et al., 2016), the outgoing and incoming radiative power densities are individually described using a gray-body radiation model with their associated emissivity/absorptivity terms. As we will see later in the article, in our experiments the emitter temperature is only a few degrees Celcius below the ambient air temperature, thus, $T_{emit} \approx T_{amb}$. In this case, we can simplify the expression for q_{rad} by performing Ta/ylor expansion around T_{amb}, resulting in,

$$q_{rad}(T_{emit}) = q_{rad}(T_{amb}) + h_{rad}(T_{emit} - T_{amb}),$$ (Equation 1)

where $q_{rad}(T_{amb})$ is the radiative cooling power density for the emitter at the ambient temperature and $h_{rad} = 4\epsilon_e \sigma T_{amb}^3$—where ϵ_e is the emitter's average emissivity, and σ is the Stefan-Boltzmann constant—is the temperature coefficient of the net radiative cooling power. $q_{rad}(T_{amb})$ typically ranges from 50 to 100 W/m^2 depending on the ambient and sky conditions (Granqvist and Hjortsberg, 1981), and $h_{rad} = 5$ W/m^2/K for a near-black emitter at $T_{amb} = 290$ K. For an emitter with an area A_e, the total net radiative cooling power is $q_{rad}(T_{emit})A_e$, as indicated in Figure 1B. The emitter also experiences additional heat transfer pathways with the ambient air. The heat transfer pathway, not through the TEG, is mainly convection, and its power density can be described using the associated heat transfer coefficient, h_e, as,

$$q_{conv} = h_e(T_{emit} - T_{amb}).$$ (Equation 2)

The heat transfer pathway through the TEG is characterized by the TEG thermal resistance, R_{TEG}. (We can safely ignore the TEG parasitic heating from the Joule heating and Peltier effects, as these effects were found to be negligible (Fan et al., 2020)) Together with the contact terms, the heat flow through the TEG is,

$$Q_{TEG} = \frac{T_{emit} - T_{amb}}{R_{TEG} + R_c + R_h}.$$ (Equation 3)

where R_c and R_h are the contact resistances at the emitter-TEG interface and TEG-heat sink interface, respectively. In Equations (1), (2), and (3), we use a positive sign to denote the emitter's outgoing heat flow. Energy balance requires $q_{rad}A_e + q_{conv}A_e + Q_{TEG} = 0$. Substituting the individual expressions for the heat transfer components allows us to solve for the temperature difference between the emitter and the ambient,

$$\Delta T = T_{amb} - T_{emit} = \frac{q_{rad}(T_{amb})A_e}{h_{rad}A_e + h_e A_e + \frac{1}{R_{TEG} + R_c + R_h}}.$$ (Equation 4)

The power generated by a TEG module can be modeled as,

$$w = c\Delta T_{TEG}^2,$$ (Equation 5)

accurate for a small temperature difference ΔT_{TEG} across the TEG, with c being the proportionality constant specific to each TEG module (Raman et al., 2019; Assawaworrarit et al., 2022).

For efficient energy harvesting, it is evident from examining Figure 1B that we need to minimize R_h and R_c. By using a high-quality heat sink and applying thermal paste at all interfaces, we can reduce the R_h and R_c to become negligible compared to R_{TEG} as reported in previous experiments (Raman et al., 2019; Assawaworrarit et al., 2022). Setting R_h and R_c to zero, we can express the temperature difference across the TEG module as,

$$\Delta T_{TEG} = \frac{q_{rad}(T_{amb})A_e}{h_{rad}A_e + h_e A_e + \frac{1}{R_{TEG}}} = \frac{q_{rad}(T_{amb})}{h_{rad} + h_e + \frac{1}{A_e R_{TEG}}},$$ (Equation 6)

and the total generated power density as,

$$w = \frac{c}{A_e}\left[\frac{q_{rad}(T_{amb})}{h_{rad} + h_e + \frac{1}{A_e R_{TEG}}}\right]^2.$$ (Equation 7)

We note that the power density here is the power generated, divided by the area of the emitter.
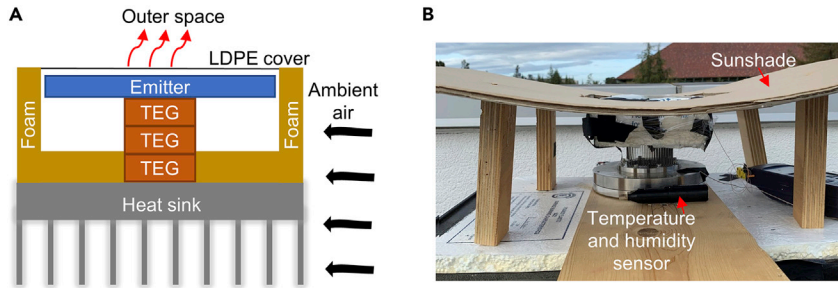
Figure 2. Experimental setup

We show a cross-section of the experimental setup in (A). We use a thermoelectric generator (TEG) as the heat engine in our experiment. The hot side of the TEG is in contact with a heat sink consisting of multiple fins, which provide good thermal contact with the ambient air. The cold side of the TEG is in contact with an emitter, which consists of an aluminum sheet covered with black tape on the top. The emitter performs radiative cooling to reach a temperature below ambient. The TEG and emitter are placed in an enclosure made of foam sheets. The top opening of the enclosure is covered with low-density polyethylene (LDPE) film. We show a photo of the setup in (B), along with a temperature-and-humidity sensor and sunshade. The sunshade prevents unwanted heating of the heat sink fins during the day, allowing continuous operation of the setup for over a week.

There are several ways to optimize the power density in Equation (7). Typically, for a given emitter at a given ambient and sky conditions, h_{rad} and $q_{rad}(T_{amb})$ are fixed. h_e is fixed by the type of emitter enclosure used. R_{TEG} and c are properties of the TEG module. In one of the scenarios, once a module with sufficiently high R_{TEG} and c values is selected, we assume that these quantities can be treated as fixed. This leaves us with A_e as the remaining design variable. Maximizing the power density expression of Equation (7) gives the optimal value for A_e,

$$A_{e,optimal} = \frac{1}{(h_{rad} + h_e)R_{TEG}}. \quad \text{(Equation 8)}$$

In certain applications, for a given TEG module, the available emitter area A_e might be too small than the $A_{e, optimal}$ as determined using Equation (8). This may occur, for example, when the total area available for radiative cooling is limited. In such cases, we can stack a number (n) of identical TEG modules. The optimization is then carried out with respect to n, keeping both A_e and R_{TEG} fixed. We rewrite Equation (7) for the total power density from all the TEGs in the stack as,

$$w_{total} = \frac{nc\left(\frac{\Delta T}{n}\right)^2}{A_e} = \frac{c}{nA_e}\left[\frac{q_{rad}(T_{amb})}{h_{rad} + h_e + \frac{1}{nA_eR_{TEG}}}\right]^2, \quad \text{(Equation 9)}$$

and the optimal number of TEGs in the stack is:

$$n_{optimal} = \frac{1}{(h_{rad} + h_e)A_eR_{TEG}}. \quad \text{(Equation 10)}$$

Thus by stacking TEGs, we gain additional design freedom to realize the maximum power density even with limited emitter area. In the experiment that follows, we demonstrate this stacking approach.

Experiment

Using the insights from the analysis above, we develop our experimental setup. In Figure 2A, we show the cross-section of our setup for nighttime power harvesting from radiative cooling. We select commercially available thermoelectric generators (Marlow TG12-4 with c = 0.16 mW/°C^2 and R_{TEG} = 2.5 K/W (Digikey)) in our experiment. We use a heat sink from a Hewlett-Packard computer for the hot side of the TEG, resulting in $R_h \sim 0.5$ K/W. We minimize various contact thermal resistances by applying silicone thermal paste at the emitter-TEG interface and the TEG-heat sink interface. We also construct an insulation enclosure for the emitter out of household foam sheets to surround the sides and bottom of the emitter while leaving space for the TEG-heat sink contact. We cover the top opening of the enclosure with low-density polyethylene (LDPE) film to provide thermal isolation and minimize the wind-induced convective transfer of the emitter from the ambient. With these arrangements, we have h_e = 5–8 W/m^2/K depending on wind and humidity,
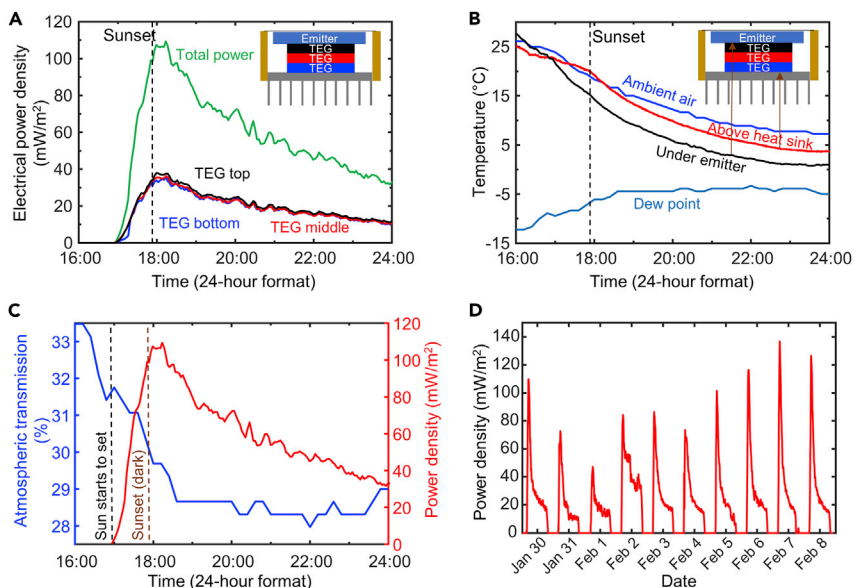
Figure 3. Nighttime electricity generation using radiative cooling

We show the generated power density and powers from individual TEGs in (A). The individual TEG power curves are color-coded according to the colors in the setup figure in the inset. The temperatures of the air, above the heat sink, and under the emitter are shown in (B), along with the dew point. As the dew point increases and air temperature decreases, the total power generated decreases as we progress through the night, reaching a peak right after the sunset. In (C), We show the reduction of atmospheric transparency at night. As the night progress, the atmospheric transparency decreases, reducing the nighttime generated power from radiative cooling. In (D), we show the multi-day power measurement data.

consistent with ref. (Raman et al., 2019; Chen et al., 2016). To achieve the maximum generated power density of Equation (10), we need $nA_e = 363$ cm^2. The emitter consists of an aluminum plate covered on the radiating side with black tape. The average emissivity of such emitter in the infrared wavelength range of 2-15 μm is 94%. We opt for an emitter area of 11 × 11 sq. cm and use a number of TEGs n = 3. This choice allows us to effectively increase the thermal resistance across the TEG of Figure 1B to a value that makes R_h negligible. Figure 2B shows the setup on a rooftop of Stanford University's Electrical Engineering Department building with unobstructed access to the sky.

We performed measurements for multiple-day periods from January to March 2022. We took separate power measurements from each individual TEG module. We used a source meter (Keithley 2635B) running maximum power point tracking to measure the power from the middle TEG. For the top and bottom TEGs, we measured the open-circuit voltages using multimeters (HP34401A and BK 2831E) and estimated the generated power from the correlation between the TEG open-circuit voltage and generated power similar to the practice in Li et al. (2018a, 2018b). We used a temperature-and-humidity sensor (Easylog EL-USB-2-LCD) to measure the ambient temperature and dew point. The sensor is placed outside the chamber, right near the heat sink as shown in Figure 2B. We used type-K thermocouples and a datalogger (Reed SD-947) to measure the temperatures at various locations in the setup.

Figure 3A shows the electrical power measurements for March 10, 2022. The individual electrical power measurements from the three TEGs, along with the total generated power, are shown on the plot. Figure 3B shows the air temperature, dew point, and temperatures across the TEG stack. The power measurements of individual TEGs are well-balanced, indicating that the TEG stack effectively captures the heat flow from the heat sink to the emitter with minimal leakage. The total generated power from the three TEGs increases as the Sun goes over the horizon, reaching 108 mW/m^2 before decreasing overnight. After the sunset, the increasing dewpoint indicates increasing water vapor density in the atmosphere. This in turn increases the relative humidity of the atmosphere, reducing the atmospheric transparency (Figure 3C). As a result, we have less thermal radiation from the emitter to outer space. The emitter temperature increases, leading to reduced power generation. Over multiple days of the experiment, we measured similar power values and trends (Figure 3D).

In summary, compared with previous studies (Raman et al., 2019), we have achieved significant improvement in the power density by adjusting the device configuration in the following aspects. First, we optimize the emitter area taking into account the tradeoff between the parasitic convection between the ambient and the emitter, and outgoing thermal radiation for radiative cooling. Second, we stack multiple TEGs to improve the thermal insulation between the heat sink and the emitter while increasing the output electrical power density. Third, we used silicone thermal paste to reduce the contact resistances (R_c, R_h). These adjustments allow us to reduce parasitic heat transfers and achieve power density exceeding 100 mW/m^2.

Conclusion

Nighttime energy harvesting using radiative cooling is a promising, simple approach to provide cheap power to resource-scarce, remote geographic places. We provide an optimization analysis of the thermal heat transfer mechanisms between different system components to maximize the generated power density and result in significant power generation at night. We demonstrate a setup with >100 mW/m^2 power generation at nighttime. Further improvement can be achieved by using a selective emitter together with an enclosure that further reduces the parasitic thermal transfer.

Limitations of the study

The high-power density at nighttime, reported in this article, is possible with a clear sky at low humidity. Furthermore, we have explored thermoelectric modules available commercially and chosen an option with a high c value (Equation 5) and high R_{TEG}. Non-commercial thermoelectric modules can potentially have both higher c and R_{TEG}, leading to a higher power at nighttime from radiative cooling.

STAR★METHODS

Detailed methods are provided in the online version of this paper and include the following:

- KEY RESOURCES TABLE
- RESOURCE AVAILABILITY
  - Lead contact
  - Materials availability

AUTHOR CONTRIBUTIONS

Z. O., S. A., L. F., W. L., and S. F. developed the theory. Z. O., S. A., W. L., and S. F. designed the experiment. Z. O. performed the experiment and data analysis. Z. O., S. A., and S. F. wrote the article, with inputs from L. F. and W. L.

DECLARATION OF INTERESTS

The authors declare no competing interests.

REFERENCES

Ajmal, T., Dyo, V., Allen, B., Jazani, D., and Ivanov, I. (2014). Design and optimisation of compact RF energy harvesting device for smart applications. Electron. Lett. 50, 111–113. https://doi.org/10.1049/el.2013.3434.

Assawaworrarit, S., Omair, Z., and Fan, S. (2022). Nighttime electric power generation at a density of 50 mW/m2 via radiative cooling of a photovoltaic cell. Appl. Phys. Lett. 120, 143901. https://doi.org/10.1063/5.0085205.

Bowen, T., Chernyakhovskiy, I., Xu, K., Gadzanku, S., and Coney, K. (2021). USAID grid-Scale energy storage Technologies Primer. Article at OSTI,10.2172/1808490.

Buddhiraju, S., Santhanam, P., and Fan, S. (2018). Thermodynamic limits of energy harvesting from outgoing thermal radiation. Proc. Natl. Acad. Sci. USA 115, E3609–E3615. https://doi.org/10.1073/pnas.1717595115.

Byrnes, S.J., Blanchard, R., and Capasso, F. (2014). Harvesting renewable energy from Earth's

mid-infrared emissions. Proc. Natl. Acad. Sci. USA 111, 3927–3932. https://doi.org/10.1073/pnas.1402036111.

Chen, Z., Zhu, L., Raman, A., and Fan, S. (2016). Radiative cooling to deep sub-freezing temperatures through a 24-h day–night cycle. Nat. Commun. 7, 13729. https://doi.org/10.1038/ncomms13729.

Deppe, T., and Munday, J.N. (2020). Nighttime photovoltaic cells: electrical power generation by optically coupling with deep space. ACS Photonics 7, 1–9. https://doi.org/10.1021/acsphotonics.9b00679. 10.1021/acsphotonics.9b00679.

Digikey. TG12-4-01LS. https://www.digikey.com/en/products/detail/marlow-industries-inc/TG12-4-01LS/6159118.

DiSalvo, F.J. (1999). Thermoelectric cooling and power generation. Science 285, 703–706. https://doi.org/10.1126/science.285.5428.703.

Dong, M., Chen, N., Zhao, X., Fan, S., and Chen, Z. (2019). Nighttime radiative cooling in hot and humid climates. Opt. Express 27, 31587–31598. https://doi.org/10.1364/OE.27.031587.

Eriksson, T.S., and Granqvist, C.G. (1982). Radiative cooling computed for model atmospheres. Appl. Opt. 21, 4381–4388. https://doi.org/10.1364/AO.21.004381.

Eriksson, T.S., Lushiku, E.M., and Granqvist, C.G. (1984). Materials for radiative cooling to low temperature. Sol. Energy Mater. 11, 149–161. https://doi.org/10.1016/0165-1633(84)90067-4.

Fan, S., and Li, W. (2022). Photonics and thermodynamics concepts in radiative cooling. Nat. Photonics 16, 182–190. https://doi.org/10.1038/s41566-021-00921-9.

Fan, L., Li, W., Jin, W., Orenstein, M., and Fan, S. (2020). Maximal nighttime electrical power generation via optimal radiative cooling. Opt Express 28, 25460–25470. https://doi.org/10.1364/OE.397714.

Granqvist, C.G., and Hjortsberg, A. (1981). Radiative cooling to low temperatures: general considerations and application to selectively emitting SiO films. J. Appl. Phys. 52, 4205–4220. https://doi.org/10.1063/1.329270.

Green, M.A., Dunlop, E.D., Hohl-Ebinger, J., Yoshita, M., Kopidakis, N., Bothe, K., Hinken, D., Rauer, M., and Hao, X. (2022). Solar cell efficiency tables (version 60). Prog. Photovolt. Res. Appl. 30, 687–701. https://doi.org/10.1002/pip.3595.

Holmes, A.S., Hong, G., Pullen, K.R., and Buffard, K.R. (2004). Axial-flow microturbine with electromagnetic generator: design, CFD simulation, and prototype demonstration. Maastricht MEMS 2004 Tech. Digest, 568–571. https://doi.org/10.1109/MEMS.2004.1290648.

Hossain, M.M., and Gu, M. (2016). Radiative cooling: principles, progress, and potentials. Adv. Sci. 3, 1500360. https://doi.org/10.1002/advs.201500360.

Hu, M., Zhao, B., Ao, X., Zhao, P., Su, Y., and Pei, G. (2018). Field investigation of a hybrid photovoltaic-photothermic-radiative cooling system. Appl. Energy 231, 288–300. https://doi.org/10.1016/j.apenergy.2018.09.137.

Ishii, S., Dao, T.D., and Nagao, T. (2020). Radiative cooling for continuous thermoelectric power generation in day and night. Appl. Phys. Lett. 117, 013901. https://doi.org/10.1063/5.0010190.

Khan, S., Kim, J., Roh, K., Park, G., and Kim, W. (2021). High power density of radiative cooled compact thermoelectric generators based on body heat harvesting. Nano Energy 87, 106180. https://doi.org/10.1016/j.nanoen.2021.106180.

Li, W., and Fan, S. (2019). Radiative cooling: harvesting the coldness of the universe. Opt. Photonics News 30, 32–39. https://doi.org/10.1364/OPN.30.11.000032.

Li, W., Shi, Y., Chen, K., Zhu, L., and Fan, S. (2017). A comprehensive photonic approach for solar cell cooling. ACS Photonics 4, 774–782. https://doi.org/10.1021/acsphotonics.7b00089.

Li, W., Shi, Y., Chen, Z., and Fan, S. (2018a). Photonic thermal management of coloured objects. Nat. Commun. 9, 4240. https://doi.org/10.1038/s41467-018-06535-0.

Li, G., Shittu, S., Diallo, T.M., Yu, M., Zhao, X., and Ji, J. (2018b). A review of solar photovoltaic-thermoelectric hybrid system for electricity generation. Energy 158, 41–58. https://doi.org/10.1016/j.energy.2018.06.021.

Li, T., Zhai, Y., He, S., Gan, W., Wei, Z., Heidarinejad, M., Dalgo, D., Mi, R., Zhao, X., Song, J., et al. (2019). A radiative cooling structural material. Science 364, 760–763. https://doi.org/10.1126/science.aau910.

Li, W., Buddhiraju, S., and Fan, S. (2020a). Thermodynamic limits for simultaneous energy harvesting from the hot sun and cold outer space. Light Sci. Appl. 9, 68. https://doi.org/10.1038/s41377-020-0296-x.

Li, Z., Chen, Q., Song, Y., Zhu, B., and Zhu, J. (2020b). Fundamentals, materials, and applications for daytime radiative cooling. Adv. Mater. Technol. 5, 1901007. https://doi.org/10.1002/admt.201901007.

Li, X., Peoples, J., Huang, Z., Zhao, Z., Qiu, J., and Ruan, X. (2020c). Full daytime sub-ambient radiative cooling in commercial-like paints with high figure of merit. Cell Rep. Phys. Sci. 1, 100221. https://doi.org/10.1016/j.xcrp.2020.100221.

Li, X., Peoples, J., Yao, P., and Ruan, X. (2021). Ultrawhite BaSO4 Paints and films for Remarkable daytime Subambient radiative cooling. ACS Appl. Mater. Interfaces 13, 21733–21739. https://doi.org/10.1021/acsami.1c02368.

Liao, T., Xu, Q., Dai, Y., Cheng, C., He, Q., and Ni, M. (2022). Radiative cooling-assisted thermoelectric refrigeration and power systems: coupling properties and parametric optimization. Energy 242, 122546. https://doi.org/10.1016/j.energy.2021.122546.

Mandal, J., Fu, Y., Overvig, A.C., Jia, M., Sun, K., Shi, N.N., Zhou, H., Xiao, X., Yu, N., and Yang, Y. (2018). Hierarchically porous polymer coatings for highly efficient passive daytime radiative cooling. Science 362, 315–319. https://doi.org/10.1126/science.aat9513.

Mandal, J., Yang, Y., Yu, N., and Raman, A.P. (2020). Paints as a scalable and effective radiative cooling technology for buildings. Joule 4, 1350–1356. https://doi.org/10.1016/j.joule.2020.04.010.

Ono, M., Santhanam, P., Li, W., Zhao, B., and Fan, S. (2019). Experimental demonstration of energy harvesting from the sky using the negative illumination effect of a semiconductor photodiode. Appl. Phys. Lett. 114, 161102. https://doi.org/10.1063/1.5089783.

Raman, A.P., Anoma, M.A., Zhu, L., Rephaeli, E., and Fan, S. (2014). Passive radiative cooling below ambient air temperature under direct sunlight. Nature 515, 540–544. https://doi.org/10.1038/nature13883.

Raman, A.P., Li, W., and Fan, S. (2019). Generating light from darkness. Joule 3, 2679–2686. https://doi.org/10.1016/j.joule.2019.08.009.

Rephaeli, E., Raman, A., and Fan, S. (2013). Ultrabroadband photonic Structures to achieve high-performance daytime radiative cooling. Nano Lett. 13, 1457–1461. https://doi.org/10.1021/nl4004283.

Shi, N.N., Tsai, C.C., Camino, F., Bernard, G.D., Yu, N., and Wehner, R. (2015). Keeping cool: enhanced optical reflection and radiative heat dissipation in Saharan silver ants. Science 349, 298–301. https://doi.org/10.1126/science.aab3564.

Tsoy, A.P., Baranenko, A.V., and Tsoy, D.A. (2018). Refrigeration systems with the night radiative cooling effect for different regimes and climatic conditions. AIP Conf. Proc. 2007, 030054. https://doi.org/10.1063/1.5051915.

Yeatman, E.M. (2004). Advances in power sources for wireless sensor nodes. In Proc. Int'l Workshop Wearable and Implantable Body Sensor Networks, pp. 20–21.

Yin, X., Yang, R., Tan, G., and Fan, S. (2020). Terrestrial radiative cooling: using the cold universe as a renewable and sustainable energy source. Science 370, 786–791. https://doi.org/10.1126/science.abb0971.

Yu, L., Xi, Z., Li, S., Pang, D., Yan, H., and Chen, M. (2022). All-day continuous electrical power generator by solar heating and radiative cooling from the sky. Appl. Energy 322, 119403. https://doi.org/10.1016/j.apenergy.2022.119403.

Zhai, Y., Ma, Y., David, S.N., Zhao, D., Lou, R., Tan, G., Yang, R., and Yin, X. (2017). Scalable-manufactured randomized glass-polymer hybrid metamaterial for daytime radiative cooling. Science 355, 1062–1066. https://doi.org/10.1126/science.aai7899.

Zhao, B., Hu, M., Ao, X., Xuan, Q., and Pei, G. (2018). Comprehensive photonic approach for diurnal photovoltaic and nocturnal radiative cooling. Sol. Energy Mater. Sol. Cells 178, 266–272. https://doi.org/10.1016/j.solmat.2018.01.023.

Zhao, D., Aili, A., Zhai, Y., Xu, S., Tan, G., Yin, X., and Yang, R. (2019). Radiative sky cooling: Fundamental principles, materials, and applications. Appl. Phys. Rev. 6, 021306. https://doi.org/10.1063/1.5087281.

Zhao, B., Pei, G., and Raman, A.P. (2020). Modeling and optimization of radiative cooling based thermoelectric generators. Appl. Phys. Lett. *117*, 163903. https://doi.org/10.1063/5.0022667.

Zhao, B., Hu, M., Ao, X., Xuan, Q., Song, Z., and Pei, G. (2021). Is it possible for a photovoltaic-thermoelectric device to generate electricity at night? Sol. Energy Mater. Sol. Cells *228*, 111136. https://doi.org/10.1016/j.solmat.2021.111136.

Zhou, L., Song, H., Liang, J., Singer, M., Zhou, M., Stegenburgs, E., Zhang, N., Xu, C., Ng, T., Yu, Z., et al. (2019). A polydimethylsiloxane-coated metal structure for all-day radiative cooling. Nat. Sustain. *2*, 718–724. https://doi.org/10.1038/s41893-019-0348-5.

Zhu, L., Raman, A., and Fan, S. (2013). Color-preserving daytime radiative cooling. Appl. Phys. Lett. *103*, 223902. https://doi.org/10.1063/1.4835995.

Zhu, L., Raman, A., Wang, K.X., Anoma, M.A., and Fan, S. (2014). Radiative cooling of solar cells. Optica *1*, 32. https://doi.org/10.1364/OPTICA.1.000032.

Zhu, L., Raman, A.P., and Fan, S. (2015). Radiative cooling of solar absorbers using a visibly transparent photonic crystal thermal blackbody. Proc. Natl. Acad. Sci. USA *112*, 12282–12287. https://doi.org/10.1073/pnas.1509453112.

STAR★METHODS

KEY RESOURCES TABLE

REAGENT or RESOURCE	SOURCE	IDENTIFIER
Other		
Weather data	This paper	On request from the contact author (shanhui@stanford.edu)
Thermoelectric power generation data	This paper	On request from the contact author(shanhui@stanford.edu)

RESOURCE AVAILABILITY

Lead contact

Further information and requests for resources should be directed to and will be fulfilled by the corresponding author, Prof Shanhui Fan (shanhui@stanford.edu).

Materials availability

The study did not generate new unique materials.

Data and code availability

- The weather data (air temperature, humidity, and wind parameters) and thermoelectric generation data (current-voltage curve in operation) are available from the corresponding author upon request.

- The paper does not report the original code.

- Any additional information required to analyze the data reported in this paper is available from the corresponding author upon request.